Chapter 32

Live Cell Imaging of Nuclear Actin Filaments and Heterochromatic Repair foci in *Drosophila* and Mouse Cells

Colby See, Deepak Arya, Emily Lin, and Irene Chiolo

Abstract

Pericentromeric heterochromatin is mostly composed of repeated DNA sequences, which are prone to aberrant recombination during double-strand break (DSB) repair. Studies in *Drosophila* and mouse cells revealed that 'safe' homologous recombination (HR) repair of these sequences relies on the relocalization of repair sites to outside the heterochromatin domain before Rad51 recruitment. Relocalization requires a striking network of nuclear actin filaments (F-actin) and myosins that drive directed motions. Understanding this pathway requires the detection of nuclear actin filaments that are significantly less abundant than those in the cytoplasm, and the imaging and tracking of repair sites for long time periods. Here, we describe an optimized protocol for live cell imaging of nuclear F-actin in *Drosophila* cells, and for repair focus tracking in mouse cells, including: imaging setup, image processing approaches, and analysis methods. We emphasize approaches that can be applied to identify the most effective fluorescent markers for live cell imaging, strategies to minimize photobleaching and phototoxicity with a DeltaVision deconvolution microscope, and image processing and analysis methods using SoftWoRx and Imaris software. These approaches enable a deeper understanding of the spatial and temporal dynamics of heterochromatin repair and have broad applicability in the fields of nuclear architecture, nuclear dynamics, and DNA repair.

Key words Live cell imaging, Nuclear actin filaments, Repair foci, DSB repair, Homologous recombination, Drosophila cells, Mouse cells

1 Introduction

Repairing double-strand breaks (DSBs) is particularly challenging in pericentromeric heterochromatin (hereafter, 'heterochromatin') given the abundance of repeated DNA sequences prone to ectopic recombination [1–4]. Heterochromatin comprises ~30% of fly and human genomes [5–7] and is characterized by high levels of silent histone marks (*e.g.*, H3K9me2/3 [6]) and associated proteins (*e.g.*, HP1a in *Drosophila* cells [8, 9], and HP1α or HP1β in mammalian

Colby See and Deepak Arya have contributed equally for this manuscript.

Andrés Aguilera and Aura Carreira (eds.), *Homologous Recombination: Methods and Protocols*, Methods in Molecular Biology, vol. 2153, https://doi.org/10.1007/978-1-0716-0644-5_32,

cells [10, 11]), but it is absent in budding yeast. In *Drosophila*, about half of these sequences are simple 'satellites' (mostly tandem 5-bp sequences) repeated for hundreds of kilobases to megabases, while the rest is made of transposable elements and about 250 isolated genes [5–7]. Mouse heterochromatin is mostly composed of the A/T-rich 'major' satellite (organized as 234 bp tandem repeats), in addition to non-LTR retrotransposons (SINEs and LINEs), endogenous retroviruses (ERVs), and other repeats [12, 13]. The high level of repeated DNA sequences associated with different chromosomes renders heterochromatin a major threat to genome stability in multi-cellular eukaryotes [1–4, 14].

DSB repair by homologous recombination (HR) relies on resection to form single-stranded DNA (ssDNA), which invades a 'donor' homologous template for DNA synthesis and repair [15]. In single-copy sequences, a unique donor is present on the sister chromatid or the homologous chromosome, and HR is mostly error-free [15]. In heterochromatin, however, the availability of up to millions of potential donor sequences can initiate unequal sister chromatid exchanges or intra-/inter-chromosomal recombination, leading to extra-chromosomal DNA circles (ECCs), deletions, duplications, translocations, and formation of dicentric or acentric chromosomes [16–21, 23]. Despite this danger, HR is a major pathway for heterochromatin repair in *Drosophila* and mammalian cells [18–20, 22–26], and studies from our laboratory and others have uncovered specialized mechanisms for 'safe' HR in this domain [18–29] (reviewed in [2–4, 14, 27, 30]).

Drosophila and mouse heterochromatin form distinct nuclear domains (a single domain in *Drosophila* and several 'chromocenters' in mouse cells) [9, 23, 31, 32], which facilitates the characterization of heterochromatic repair pathways using cytological approaches. Early studies in *Drosophila* cells revealed that HR starts inside the domain with resection (Fig. 1), while strand invasion is temporarily halted [18, 19, 23]. SUMOylation by the Smc5/6 subunits Nse2/Cerv and Nse2/Qjt, and by dPIAS, is responsible for the initial block to HR and for relocalization of repair sites to the nuclear periphery [18, 19, 23]. Repair sites associate with nuclear pores or Koi/Spag4 inner nuclear membrane proteins (INMPs) at the nuclear periphery, where repair continues with Rad51 recruitment [18, 20, 23]. Relocalization also requires a remarkable network of dynamic nuclear actin filaments originating at heterochromatic repair sites and reaching the nuclear periphery [20, 30]. Myosins associated with repair sites drive movement through their ability to 'walk' along the filaments [20]. Similar pathways relocalize heterochromatic DSBs in mouse cells, where repair appears to continue at the chromocenter periphery [20, 26, 33, 2]. Relocalization defects result in aberrant recombination and widespread genomic instability, revealing the importance of these dynamics for genome integrity [18–21, 23]. Relocalization likely promotes "safe" HR repair while preventing aberrant

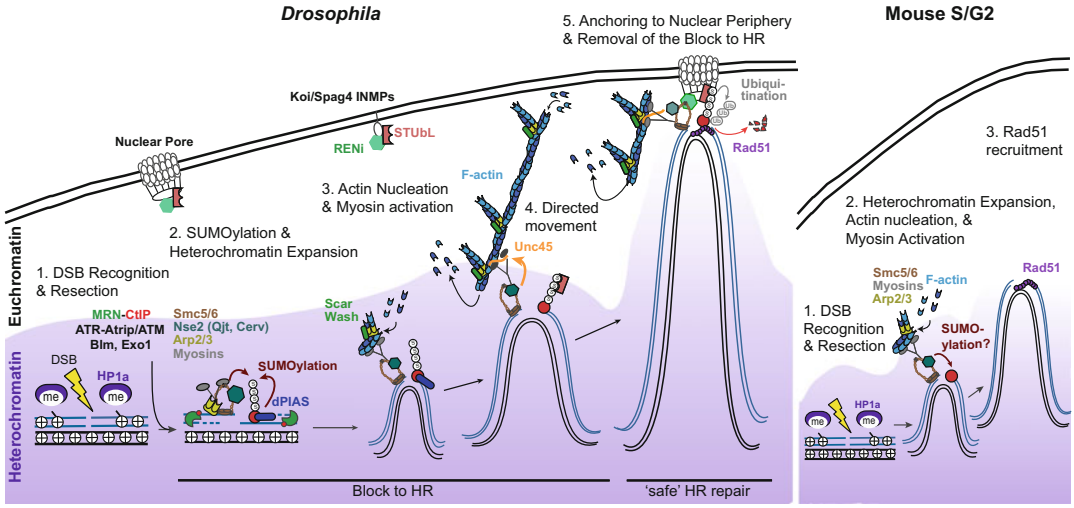

Fig. 1 Model describing the heterochromatin repair pathway in *Drosophila* and mouse cells. In *Drosophila* cells, DSBs are promptly recognized inside the heterochromatin domain, leading to resection by Mre11, CtIP, Exo1, Blm, and Dna2, and to activation of checkpoint kinases (particularly ATR) [23]. Resection and checkpoint activation promote heterochromatin expansion [23]. Smc5/6 (specifically its SUMO-E3 ligase subunits Nse2/Qjt and Nse2/Cerv) and the SUMO-E3 ligase dPIAS, induce the block to HR progression and relocalization [23]. Myo1A, Myo1B and MyoV nuclear myosins and Arp2/3 actin nucleator are recruited to heterochromatic DSBs *via* HP1a and the MRN complex (Mre11-Rad50-Nse2) [20]. Scar or Wash-dependent Arp2/3 activation promotes nuclear actin filament assembly at repair sites [20], with polymerization largely occurring at the periphery of the heterochromatin domain [20]. Unc45 recruitment by Smc5/6 activates nuclear myosins that 'walk' along the filaments and interact with Smc5/6, enabling directed motion of repair sites to the nuclear periphery [20, 21, 42]. STUbL/RENi protein complexes are associated with the nuclear periphery to promote DSB anchoring and repair progression [18], likely *via* STUbL-dependent ubiquitination of SUMOylated targets and activation or degradation through the proteasome. HR progresses with Rad51 recruitment and strand invasion using the homologous chromosome or the sister chromatid [20, 25]. Similarly, in mouse G2 cells, heterochromatin expands in response to damage [26, 69], and Rad51 is recruited after relocalization of repair sites to outside the chromocenters [26, 33, 20]. Relocalization requires resection, Smc5/6, Arp2/3, actin polymerization, and myosins' ability to walk along actin filaments [20, 26]. INMPs: Inner Nuclear Membrane Proteins

recombination, by isolating DSBs and their repair templates (on the sister chromatid or homologous chromosome [20, 25]) away from ectopic sequences before strand invasion.

Understanding these spatial and temporal dynamics requires the ability to visualize repair components, heterochromatin domains, and nuclear F-actin, by live cell imaging. Repair sites can be detected by fluorescent tagging of repair components that form cytologically visible foci upon recruitment to DSBs [18, 20, 34–42, 23]. For example, Mdc1 (*Drosophila* Mu2) is associated with the phosphorylated form of the histone variant H2Av [23, 43, 44] (γH2Av, corresponding to mammalian DSB mark γH2AX [40, 45, 46]), and mediates the recruitment of other HR proteins [47–50]. Thus, Mu2/Mdc1 foci can be used as a marker of repair

sites during early and late steps of HR repair [18, 20, 21, 23, 42]. Similarly, fluorescent tagging of HP1 proteins enables the detection of heterochromatin domains [18–20, 23]. Relocalization occurs over a time span of one hour or longer, and a specific challenge of these studies is imaging the samples over long time periods with sufficient time points and Z-stacks to enable focus tracking, while limiting phototoxicity and photobleaching effects [42]. Imaging nuclear F-actin introduces additional challenges because cytoplasmic F-actin is typically more abundant than its nuclear counterpart, interfering with the detection of nuclear signals *via* traditional staining and imaging approaches [51, 52]. Major breakthroughs resulted from the development of fluorescently tagged F-actin-specific probes with nuclear localization signals (NLS) for live imaging of nuclear filaments [20, 30, 51, 53–55].

Here, we describe a procedure for live cell imaging of damage-induced nuclear F-actin in *Drosophila* cells, and of repair foci in mouse cells, including: (1) the generation of cell lines expressing fluorescent markers for nuclear F-actin, repair foci, and heterochromatin domains; (2) how the same fields are imaged before and after IR; (3) the setup used to minimize light exposure with a DeltaVision deconvolution microscope system; (4) post-image processing with SoftWoRx software, which maximizes information recovery from low-exposure experiments; and (5) focus tracking and motion analysis in mouse cells. Together, these techniques enable studying the spatial and temporal dynamics of heterochromatin repair, which cannot be accomplished with fixed cell studies or biochemical approaches. Similar approaches are broadly applicable to the study of nuclear dynamics of repair foci in other contexts, from yeast to human cells.

2 Materials

2.1 Tissue Culture Media

(a) *Drosophila* Kc cells are maintained in Schneider's medium (Sigma) supplemented with 10% fetal bovine serum (FBS) (Gemini, GemCell) and 2% antibiotic–antimyotic (Gibco).

(b) Mouse NIH3T3 cells are maintained in DMEM medium with high glucose (VWR) supplemented with 10% calf bovine serum (CBS) (Colorado Serum Company) and 1% penicillin–streptomycin solution (Sigma). Trypsin (VWR) is used to dislodge the cells for passaging. FluoroBrite DMEM (Thermo Scientific) supplemented with 10% CBS is used during live imaging to reduce autofluorescence.

2.2 Plasmids

(a) Plasmids for *Drosophila* cells: pCopia-F-actCB-GFP-NLS was described in [20]. The original plasmid expressing the F-actin

chromobody (CB) is from Chromotek. pCopia-mCherry (mCh)-HP1a was described in [23]. pCopia-mCitrin-HP1a and pCopia-mCerulean-HP1a were generated by substituting mCh with mCitrin or mCerulean fluorescent tags, in pCopia-mCh-HP1a [23]. Plasmids containing a selection cassette were pCoPuro [56] or pCoHygro (Invitrogen).

(b) Plasmids for mouse NIH3T3 cells: pCMX-GFP-Mdc1 (kind gift from Stephen Jackson) was described in [57, 58]. pEGFP-C1-RFP-HP1α (kind gift from Peter Hemmerich) was described in [59].

2.3 Transfection Methods

(a) For *Drosophila* cells, Cellfectin II (Invitrogen) has consistently delivered the highest transfection efficiency [42] and is our agent of choice for transient transfection followed by live cell imaging. For stable cell line generation, Transit-Insect (Mirus) or Transit-2020 (Mirus) has also been used with excellent results [42] (*see* **Note 1**). 150 μg/ml hygromycin (VWR) or 300 μg/ml puromycin (VWR) was added to the media for cell selection.

(b) For Mouse NIH3T3 cells, stable cell lines have been generated using Lipofectamine 3000 (Fisher), following the manufacturer's instructions. 100 μg/ml G418 (Millipore) is added to the media for cell selection. Transient transfection was done by electroporation.

2.4 Microscopy Supplies

(a) Chambered coverslips for live imaging are from Nunc (Lab-Tek II Chambered Coverglass, Thermo Scientific).

(b) We use immersion oil with a refractive index of 1.512 (GE Healthcare). This needs to be optimized for different imaging setups, based on objectives, temperature conditions, and coverslip thickness, to reduce refraction and minimize spherical aberrations while maximizing contrast [42].

2.5 Coverslip Coating Reagents

(a) Concanavalin A (ConA) Type VI (Sigma) works better than other coating agents for immobilizing *Drosophila* cells [42] on the coverslip.

(b) Coating for mouse NIH 3T3 is done with fibronectin (Sigma).

2.6 Microscope Hardware

The procedure described here uses a DeltaVision Elite deconvolution inverted microscope (Applied Precision/GE Healthcare). The microscope is equipped with white light LED (rated 100 Lumens at 350 mA), seven-color InsightSSI solid-state illumination system, PlanApo 60× oil objective with N.A. 1.42, Ultimate Focus module, and a Coolsnap HQ2 camera [42].

2.7 Software for Image Analysis

(a) SoftWoRx (v. 6.1.3, Applied Precision/GE Healthcare) is used to control the microscope and for image processing.

(b) Imaris (v. 9.2, Bitplane, including Track+XT module, MeasurementPro, and Batch module) is used for cell registration and repair focus tracking.

(c) Customized scripts for calculation of the Mean Square Displacement (MSD) and Long-lasting Directed Motions (LDMs) have been described in [42].

2.8 X-Ray Irradiator

Cells are exposed to X-rays to induce DNA damage using an X-RAD iR-160 irradiator (Precision X-ray).

3 Methods

Successful analysis of nuclear F-actin or repair foci relative to other nuclear structures requires the optimization of different steps: (1) selecting the brightest and most photo-resistant combination of fluorescent tags for live cell imaging; (2) using microscopes that mitigate the risk of cell damage; and (3) identifying imaging conditions and post-imaging de-noising approaches to recover image details while minimizing light exposure. Additional steps for repair focus tracking include cell immobilization pre-imaging and nucleus registration post-imaging to isolate focus dynamics from cell dynamics. Once positional data are collected, MSD can be calculated to determine the biophysical properties of focus motion [42]. Here, we describe the methods we have implemented for fluorescent imaging of damage-induced nuclear F-actin in *Drosophila* cells, and repair focus analysis in mouse cells. Methods for focus tracking, MSD analysis, and detection of LDMs in *Drosophila* cells have been previously described [42].

3.1 Live Cell Imaging of Damage-Induced Nuclear F-Actin in Drosophila Cells

Live cell imaging of nuclear F-actin in response to IR is done in stable cell lines expressing a chromobody (a single-chain antibody) that recognizes F-actin, and tagged with mGFP and a nuclear localization signal (SV40 NLS) (*i.e.,* F-actCB-GFP-NLS [20]). Cells are typically transfected with a plasmid expressing the chromobody and a marker for repair sites, heterochromatin, or nuclear periphery, to visualize filaments relative to these nuclear structures. Notably, F-actin probes can potentially alter filament stability [52], and need to be carefully tested in the cell line of interest and potentially under different promoters. Under pCopia promoter, the F-actin chromobody enables visualization of nuclear F-actin without toxic effects for the cells or altered nuclear actin levels [20]. Additionally, the kinetics of nuclear F-actin formation and resolution in response to DNA damage have been confirmed using direct staining with phalloidin [20], ruling out secondary effects of

the visualization tool on filament formation or stability. Other probes we tested under pCopia promoter (*i.e.,* Lifeact [60], F-tractin [61], Utr230 [51, 62]) had toxic effects in Kc cells or resulted in filament stabilization and were not further used in our experiments.

3.1.1 *Drosophila Kc Cell Maintenance*

Drosophila Kc cells are split every 3–5 days to keep the culture growing exponentially at a concentration of 1.5–9 × 10^6 cells/ml, and they are split 2 days before transfection (*see* **Note 2**). These cells are semi-adherent and can easily be dislodged from the substrate by pipetting.

3.1.2 *Selection of Fluorescent Tags for Live Cell Imaging*

Live cell imaging experiments are critically dependent on selecting the best combination of fluorescent tags to maximize signal detection and minimize photobleaching throughout the time course. We have successfully used several fluorescent tags for live imaging of *Drosophila* cells (*i.e.,* EGFP, GFP, mEGFP, mCitrin, mCerulean, mTurquoise2, mCherry, Aquamarine), while others delivered poor performance (*e.g.,* E2Crimson) with our imaging setup. mEGFP or EGFP tags are the brightest and most resistant to photobleaching, and have been the best choice for the detection of weak signals (*e.g.,* nuclear F-actin [20]), and for long term imaging (*e.g.,* 4D tracking of repair foci [18]). mCherry is also quite bright and photobleaching-resistant, and is suitable to detect abundant proteins or large nuclear structures, such as the heterochromatin domain (*e.g.,* with mCh-HP1a), the nuclear periphery (*e.g.,* with mCh-LaminC), or repair foci for limited time points (*e.g.,* with mCh-Mu2/Mdc1 or mCh-TopBP1) [18–20, 23]. We established the brightness and extent of bleaching of different tags in *Drosophila* cells and our imaging conditions, by co-expressing in cultured cells HP1a carrying different fluorescent tags. For example, we used the following procedure to compare the performance of mCh, mCitrin, mCerulean, and mTurquoise2 (Fig. 2).

1. Express tagged proteins of interest by transient transfection using Cellfectin II. Transfections are performed following manufacturer's instructions in six-well plates, using 2.5 μg of each plasmid. Following this procedure, most cells expressing one plasmid also express the other two, and co-transfected proteins are expressed at similar levels. We co-expressed mCh-HP1a, mCitrin-HP1a, and mCerulean-HP1a or mTurquoise2-HP1a with tags identically positioned in the fusion protein.
2. Cells expressing all three tags are imaged with exposure conditions aiming to identical max target intensity for each wavelength, and similar to those planned for live imaging. For 3-color imaging, select the filter set and position the polychroic mirror for imaging YFP/mCh/CFP (*see* **Note 3**).

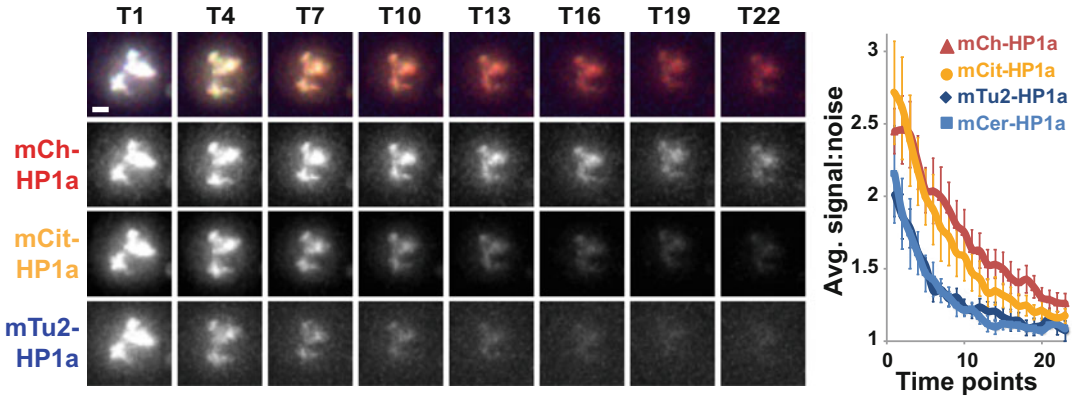

Fig. 2 Fluorescent tag testing in *Drosophila* cells. Image of one cell and quantification of the average signal-to-noise ratio over time in a population of cells expressing mCh, mCitrin (mCit) and mTurquoise2 (mTu2)-tagged HP1a, imaged for 23 time points every 1 min 15 s, using 2 × 2 binning of the camera, 32% light transmittance in each channel, and exposure of 2 ms for mTu2/mCer/mCh and 4 ms for mCit, corresponding to a target intensity of 400 (a.u.) at time point 0. Quantification of signal intensity relative to the background shows the extent of photobleaching over time. Images are snapshots of volume reconstructions. Scale bar = 1 μm. $n = 4$ cells for mTur2 and mCit, and $n = 8$ cells for mCh and mCit. Error bars: SEM

3. After deconvolution and volume reconstruction *see* Subheadings 3.1.8 and 3.1.9), the fluorescent intensity for each channel is measured using SoftWoRx "Data Inspector" function in "Tools", with an area of 4 pixels across the HP1a domain. Intensity values are measured across different cells and time points, to establish signal resistance to bleaching (Fig. 2). This analysis shows that mCh and mCitrin are brighter and more photoresistant than mTurquoise2 or mCerulean. mCh is more photoresistant than mCitrin.

3.1.3 Generation of Stable Drosophila Cell Lines Expressing the F-actin Chromobody and mCh-HP1a

1. Cells are transfected with Cellfectin II using 2.5 μg of each plasmid expressing the protein of interest (F-act-CB-GFP-NLS and mCh-HP1a) and 1 μg of plasmid carrying a selection cassette (pCoPuro or pCoHygro) (*see* **Notes 4** and **5**).
2. Cells are transferred to fresh media containing the selection agent 3–4 days following transfection.
3. Cells are split as needed to maintain an exponentially growing culture during selective pressure, and they are tested after 4+ weeks for protein expression.

3.1.4 Coating of Chambered Coverslips for Kc Cell Immobilization

Cells are immobilized on chambered coverslips using a coating procedure to minimize rotational and translational movements during live cell imaging. Follow this procedure for coating:

1. Prepare a solution of 1 mg/ml ConA in water. Stir until ConA is mostly dissolved, then filter the solution with a 0.22 μm pore-size filter.

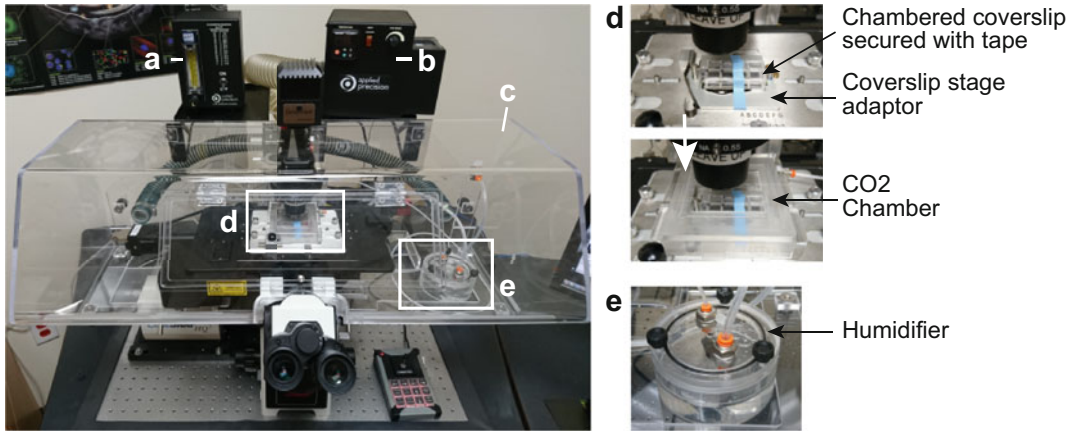

Fig. 3 Microscope environmental chamber setup for live cell imaging. The environmental chamber maintains a constant temperature, humidity, and CO_2 concentration for live cell imaging. The setup includes: (**a**) a Flowmeter to regulate CO_2 flow; (**b**) a temperature regulator; (**c**) the environmental chamber enclosure; (**d**) a stage holding the chambered coverslip, shown with or without the CO_2 chamber for local CO_2 regulation; (**e**) a humidifier connected to a CO_2 chamber. CO_2 regulation is used for mouse cells and not for *Drosophila* cells

2. Add ~100 μl of ConA solution to each well of the eight-well chambered coverslip. The solution should form a thin coating on the surface of the well. Allow the solution to dry in the tissue culture hood with the lid of the coverslip off. Additional coating may be applied if necessary by repeating **step 2**. Use the coated coverslips within 1 week after preparation for better results.

3.1.5 Temperature Regulation for Live Imaging of Kc Cells

To ensure consistent imaging during a time course, we use an environmental chamber mounted around the microscope that maintains a constant temperature (Fig. 3). This helps maintain a healthy culture and reduces shifts of the stage during the imaging procedure. For *Drosophila* cells, the chamber is turned on ~10 min before starting the experiment and the temperature is maintained at 25 °C throughout the experiment.

3.1.6 Image Acquisition Setup and Imaging of Untreated Kc Cells

The following procedure for live imaging of nuclear F-actin is optimized for cells expressing F-act CB-GFP-NLS and mCh-HP1a with a DeltaVision Elite deconvolution inverted microscope (*see* **Note 6**).

1. Split cells to a density of 2×10^6 cells/ml 2 days before the experiment.
2. On the day of imaging, pellet ~200 μl of cells in a 1.5 ml tube, by spinning at 200 × *g* for 3 min. Remove and discard 150–180 μl of supernatant to increase the concentration of the cells and gently resuspend the cells in the remaining volume by pipetting.

3. Transfer the cells to a corner of a well of the chambered coverslip. Let the cells settle for 10–15 min before imaging (*see* **Note 7**). Meanwhile, set the temperature of the microscope's environmental chamber to 25 °C.
4. Add 150–180 μl of fresh media to the well without disturbing the cells.
5. On the microscope, manually position the 60× objective and the dichroic filter for imaging GFP/mCh. Select the corresponding filter set option for live imaging under "Resolve3D Settings," "Misc," and "Live Cell" in the drop down menu for "Excitation," "Emission," and "Eyepiece" filter sets. Click on "Activate Filter Sets".
6. Place a drop of immersion oil on the objective lens.
7. Place the chambered coverslip on the stage adaptor and secure it tightly using tape (Fig. 3 and [42]).
8. Place the adaptor/chambered coverslip on the stage of the microscope and adjust the stage level so that the cells are in focus.
9. To minimize photobleaching, set the Coolsnap HQ2 camera to 2 × 2 binning. This reduces the resolution but results in higher light intensity collected per pixel. With this setting, it is also necessary to set the image size to max 512 × 512 px.
10. Select the fields of interest. Fields are selected based on the distribution of cells as a monolayer in addition to having a strong mCh-HP1a signal. The chromobody used to image nuclear F-actin is an antibody; thus, its signal-to-noise ratio is highly dependent on its concentration in the nuclei. Excessive chromobody expression results in too much background, while excessively low levels yield too little signal. An optimal amount of chromobody is typically found in cells characterized by strong nuclear expression and low cytoplasmic signal (Fig. 4). We select 15–20 fields/experiment. Once a field is selected, save its coordinates using the "Mark Point" option in SoftWoRx's "Point List" section.
11. Optimize the imaging path by applying the "Optimize List" option followed by the "Compact List" option in the "Point List" section. This will minimize the time spent moving from field to field, which enables imaging more fields in the available time intervals.
12. Since the same cells are imaged after damage induction by IR, it is critical to select a reference field on the coverslip that can be easily identified to adjust field coordinates for minor stage movements after returning the coverslip to the microscope (*see* Subheading 3.1.7, **step 2**). We typically use the corner of the chamber as a landmark (see Subheading 3.1.7, **step 2** and

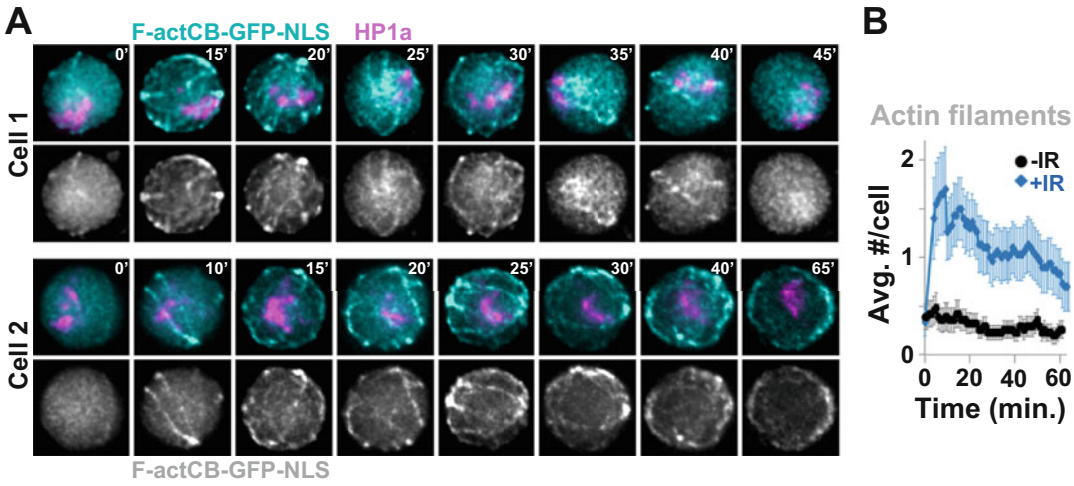

Fig. 4 IR treatment induces dynamic nuclear actin filaments. (**a**) Examples of damage-induced nuclear F-actin in *Drosophila* cells expressing F-actCB-GFP-NLS and mCh-HP1a show dynamic actin filaments mostly between 0 and 60 min after IR. Images are selected time points from volume reconstructions. Scale bar = 1 μm. (**b**) Quantification of dynamic filaments show the average number of filaments in cell treated (+) or non-treated (−) with IR. Timepoints are after IR. Reproduced with permission from Springer Nature [20]. $P < 0.0001$ for + vs −IR; $n > 25$ cells/experiment

[42] for details). This landmark should also be saved in the point list for subsequent reference.

13. Select exposure times for a given percentage of transmitted light to detect sufficient signal with minimal exposure, thus minimizing photobleaching and phototoxicity effects. For our experiments, we typically use 32% transmittance for mCh and GFP, and exposure times of 50 ms for GFP and 63 ms for mCh. This results in image underexposure, and most details are recovered by deconvolution and photobleaching correction post-imaging [42].
14. Adjust the number of Z-stacks to image the sample across its entire thickness. For *Drosophila* cells, imaging 11 Z-stacks at a 0.8 μm distance between stacks enables imaging the entire sample with sufficient resolution along the Z stack.
15. Verify each field is still in focus after selecting all the fields, by visiting each field. If necessary, readjust the focus for each frame and save the new position in the "Point List".
16. List the fields of interest in the "Design/Run Experiment," "Points" tab, "Visit Point List" section.
17. Select the "Ultimate Focus" option with five iterations in the "Visit Point List" section. This will ensure that the cells remain in focus throughout the experiment. The Ultimate Focus module uses an infrared laser-based system that detects the coverslip's position relative to the sample, thus correcting axial drifts that might occur during imaging. If this option is not available,

manual focus adjustments may be required throughout the experiment.

18. Start image capturing using the "Run" option in the "Design/Run Experiment" section. This set of images will be the 'untreated' time point (0′ in Fig. 4).
19. Deselect the "Point List" and image the landmark field.

3.1.7 IR Treatment and Imaging of Irradiated Kc Cells

After IR exposure, frame coordinates and focus might need to be adjusted as described below. The procedure takes ~5–10 min depending on the number of fields of interest.

1. Carefully remove the chambered coverslip/adaptor from the microscope without shifting the position of the stage. Take the sample to an X-ray irradiator. For our experiments, we typically expose *Drosophila* cells to 5 Gy IR, which corresponds to 44 s exposure using an X-RAD iR-160 with the stage positioned at level 30 (30 cm away from the X-ray source).
2. After IR exposure, carefully place the coverslip/adaptor back on the microscope stage. Identify the reference/landmark field using its saved coordinates from the "Point List" window, and compare to the reference image. If the stage has shifted, find the original landmark and mark the point again. Compare the coordinates of both reference points (before and after IR) to determine how much the stage has moved along the X- and Y-axes. For example, if the stage has shifted +200 μm along the X-axis and + 400 μm along the Y-axis after IR, each field of interest will need to be moved −200 and −400 μm along the X- and Y-axes, respectively. Readjust the focus of each field and save the new position of each marked point (*see* also [42]).
3. Adjust the "Image Capturing" parameters of the "Experiment Setup" option to collect images every 5 min for 1 h. In SoftWoRx, the options can be found under the "Timelapse"'section of the "Design/Run Experiment" window. Ensure that all points of interest are listed in the "Visit Point List" line of the "Points" tab on the "Design/Run Experiment" window, and that the corresponding checkbox is marked. Start the imaging process by clicking on the green arrowhead, and let the system acquire all 'treated' time points.

3.1.8 Image Processing with SoftWoRx for Nuclear F-Actin Detection

Post-image processing allows the recovery of significant image details in low-exposure images (*see* also [42]). All the following steps can be found under the "Process" tab in SoftWoRx: we apply equalization functions to correct for modest photobleaching, and deconvolution to correct the image for diffraction and aberration of light passing through the microscope optics. Deconvolution corrects for image deblurring and reduces noise, thus improving image resolution and contrast. Deconvolved images are processed

for 3D volume reconstructions to facilitate filament detection and quantification (Fig. 4a).

1. In SoftWoRx, combine the 'untreated' and 'treated' files using the "Image Fusion" function with the "Combine time points for like wavelengths" option. Save the fused file.
2. Correct the fused file for modest photobleaching using the "Equalize Time Points" function. Save the equalized file.
3. Deconvolve the equalized file using the "Deconvolve" function for ten iterations and the "Aggressive" algorithm option. This provides enough contrast to detect filaments over the background as empirically established (*see* **Note 8**).
4. In the "View" tab, select "Volume Viewer" and select "360 Around Y" in the "Move Options" section to generate a volume of each cell of interest.

3.1.9 Quantification of Actin Filaments

Here we describe the procedure we apply to quantify the number of actin filaments appearing during a 1 h kinetic. Filaments can also be quantified relative to other nuclear structures (*e.g.,* nuclear periphery, DNA repair sites, or the heterochromatin domain) (*see* [20]).

1. Zoom in on the cell of interest and visualize the GFP channel in gray to maximize the contrast, by deselecting the color checkbox under the "View" tab of the processed movie window. Adjust brightness and contrast as needed to optimize the detection of nuclear signals.
2. Turn on the "Interpolate Zoom" function in the "Display" tab under "Options," to smooth the image and facilitate filament detection over background signals.
3. Take note of each filament appearing throughout the kinetic, including the number of time points it persists, and whether it is dynamic or static across the kinetic. 'Static' actin filaments are typically unchanged in response to damage, and might participate in nuclear functions other than damage response (reviewed in [30]). Filaments responding to DNA damage tend to be very dynamic [20].
4. Average the number of dynamic filaments per cell across each time point and plot dynamic filament count/cell over time (Fig. 4b).

3.2 Live Cell Imaging of Heterochromatin and Repair Foci in Mouse Cells

Live cell imaging of repair foci relative to heterochromatin domains in mouse cells is done in NIH3T3 cells expressing GFP-tagged markers of repair foci (*e.g.,* GFP-Mdc1) and mCh- or RFP-tagged markers for heterochromatin (*e.g.,* RFP-HP1α) (*see* **Notes 9** and **10**).

3.2.1 NIH3T3 Cell Maintenance

Cells are maintained in exponential phase by splitting them every 3 days in fresh media and are incubated at 37 °C with 5% CO_2 concentration. At each passage, 10^5 cells/ml are seeded in one well

of a 6-well plate (2.5 ml of medium). Cell density is maintained at ~2–5 × 10^5 cells/ml.

3.2.2 Generation of Stable NIH3T3 Cell Lines for Live Cell Imaging

It is convenient to generate stable cell lines for live cell imaging of heterochromatic repair foci in mouse cells. *See* **Note 10** for an alternative method using transiently transfected cells.

1. To generate stable cell lines, cells are seeded in a 6-well plate at 75% confluency (~3 × 10^6 cells/ml) 12 h before transfection.
2. Cells are transfected with 1.7 μg of pCMX-GFP-Mdc1 and 0.8 μg pEGFP-C1-RFP-HP1α plasmids. G418 is added after 3 days for cell selection.
3. Cells are split every 4–5 days for 30 days, and checked once/week by live imaging ± IR to test the expression of tagged proteins and repair focus formation.

3.2.3 Coating of Chambered Coverslips for NIH3T3 Cells Immobilization

When characterizing the dynamics of DSBs in mammalian cells, it is critical to immobilize the cells on the chambered coverslip to minimize rotational and translational motions during live cell imaging, using fibronectin.

1. Prepare a solution of 100 μg/ml fibronectin in 1× PBS.
2. Add ~50 μl of the fibronectin solution to each well of the chambered coverslip and spread it on the surface. Allow the solution to dry in the hood with the lid of the coverslip off for ~2 h at RT in laminar hood.
3. Rinse the wells with 1× PBS. Use the coated coverslips within 1 week after preparation for better results.

3.2.4 Temperature and CO_2 Regulation for NIH3T3 Cells

It is important to maintain a constant temperature of 37 °C and 5% CO_2 concentration during live cell imaging of mammalian cells to ensure consistent imaging conditions and good cell health. The temperature regulator is turned on 30 min before imaging and the 5% premixed CO_2 (5% CO_2, 95% air) is turned on 5 min before imaging. The system is equipped with a CO_2 humidifier connected to a CO_2 chamber that is placed above the chambered coverslide during imaging. This maintains optimal pH and humidity values during live cell imaging (Fig. 3).

3.2.5 Image Acquisition Setup and Imaging of Untreated NIH3T3 Cells

Live cell imaging conditions need to be optimized for each tagged protein to minimize photobleaching and phototoxicity while obtaining sufficient signal for long-term focus tracking. The following procedure is optimized for cells stably expressing RFP-HP1α and GFP-Mdc1, and imaged with the DeltaVision deconvolution microscope.

1. Split cells to a density of 2 × 10^5 cells/ml 3 days before the experiment. Seed them at the same concentration in the

chambered coverslip the day before the experiment, in 400 μl fresh 10% DMEM medium.

2. To reduce the autofluorescence coming from the media, substitute DMEM with 400 μl FluoroBrite DMEM supplemented with 10% CBS 30 min before the experiment.
3. Follow the protocol described for *Drosophila* cells (Subheading 3.1.6, **steps 5–19**), except 10–15 fields that are selected for imaging. We typically use 10% transmitted light for RFP and GFP with exposure times of ~15 and 30 ms, respectively. Additionally, 10 Z stacks at a 0.95 μm distance between stacks enable imaging the entire nucleus with sufficient resolution. This set of images will be the 'untreated' time point.

3.2.6 IR Treatment and Imaging of Irradiated NIH3T3 Cells

After IR exposure, frame coordinates and focus might need to be adjusted to precisely re-center the same frames of cells imaged before IR. This procedure takes ~5–7 min depending on the number of fields of interest.

1. Carefully remove the chambered coverslip/adaptor from the microscope and expose to IR as described in Subheading 3.1.7, **step 1**. We typically use 1 Gy IR for NIH3T3 [63], corresponding to 9 seconds exposure at stage level 30 in the X-RAD iR-160 irradiator.
2. After IR exposure, carefully place the coverslip/adaptor back on the microscope stage and take an image at coordinates corresponding to the reference point. Adjust frame coordinates and focus of each field as described in Subheading 3.1.7, **step 2** and [42].
3. Adjust the "Image Capturing" parameters of the "Experiment Setup" option (as in Subheading 3.1.7, **step 3**). Collect images at least every 7 min for 203 min (30 frames) for MSD analyses, and every 2 min for at least 178 min (90 frames) for LDM analyses. This set of images will be the 'treated' time points.

3.2.7 Image Processing with SoftWoRx for Heterochromatic Repair Foci

Post-image processing (equalization and deconvolution) is used to recover significant image details in low-exposure movies [42], as described in Subheading 3.1.8.

1. In SoftWoRx, combine the 'untreated' and 'treated' files using the "Image Fusion" function with the "Combine time points for like wavelengths" option. Save the fused file.
2. Correct the fused file for modest photobleaching using the "Equalize Time Points" function. Save the equalized file.
3. Deconvolve the equalized file using the "Deconvolve" function for five iterations and the "Conservative" algorithm option. This approach provides enough contrast to distinguish repair foci and heterochromatin domains, as empirically established.

3.2.8 Cell Selection for Focus Tracking

To facilitate the processing steps required for cell registration and tracking, we recommend selecting cells that display minimal rotational/translational movement, do not contain more than 10 repair foci prior to IR, and maintain enough signal for HP1α and Mdc1 to enable distinguishing these structures from the background until the end of the kinetic. These cells are cropped from the field to reduce the file size for Imaris-related analyses. Cells in S phase contain a large number of replication-induced Mdc1 foci, which complicate detection and analysis of IR-induced foci. These cells are typically excluded from our live imaging studies.

3.2.9 Cell Registration with Imaris

After cropping the selected cells, we use Imaris to correct minor cell and/or nucleus movement ('registration') and track foci for motion analyses. Registration of mouse cells can be performed by tracking the chromocenters, which remain largely static throughout the kinetic, and by correcting cell drift using these as a reference (Fig. 5a). Alternatively, registration can be done by tracking 7+ 'static' repair foci, as previously described for *Drosophila* cells [42]. This second method is significantly more time consuming in mouse cells, given that the high number of repair foci can result in several ambiguous tracks requiring manual corrections. However, tracking repair foci rather than chromocenters for registration might be necessary for long kinetics (such as those applied to the study of LDMs [20, 42]), in which the RFP-HP1α signal might suffer excessive photobleaching by the end of the kinetic.

1. *File cropping.*

   Remove the first time point ('untreated') at this stage of the analysis using the "Crop Time" function in Imaris. The first time point does not contain IR-induced foci, so it cannot be used for focus tracking. It also typically retains some X–Y shift relative to all the other time points, as it was collected before removing the sample from the stage for IR, which can also affect the registration process. Save the cropped file with a new name to use this for further analyses. Keeping the original file is also important, as it contains information about which repair foci are present before IR. These can be used for registration but not for tracking.

2. *Automated chromocenter tracking for registration.*

   Chromocenter tracking is done using the Imaris "Spot Detection Tool", and the tracked HP1 domains are used to register the nucleus. Apply the following steps to generate the tracks, clicking the right pointing blue arrow to proceed through each step:

   (a) Generate a new "Spot" in Imaris. Select the "magic wand" icon, and click on "Rebuild".

   (b) Select the "Track Spots Over Time" box.

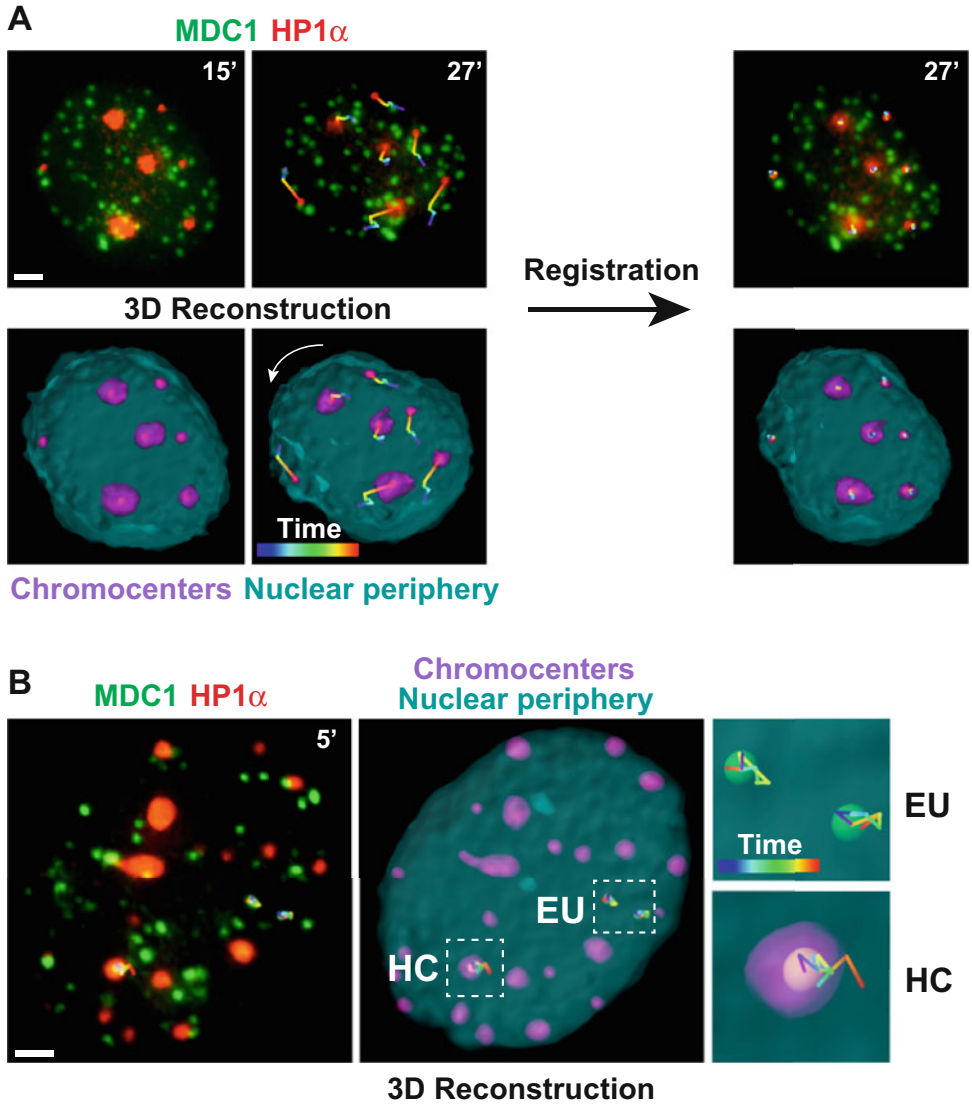

Fig. 5 Example of NIH3T3 mouse cell registration and tracking with Imaris. (**a**) Images and 3D reconstructions with Imaris show an example of an NIH3T3 cell undergoing extensive translational and rotational movement (white arrow) during live imaging over 12 min and 7 time points (the first time point is 15 min after IR, and images were taken every 2 min). Chromocenter tracking and registration corrects for this drift. (**b**) Mdc1 focus tracking after registration of NIH3T3 cells shows an example of the movement of heterochromatic (HC) and euchromatic (EU) Mdc1 foci after IR. Images were taken every 7 min for 30 time points (the first time point is 5 min after IR). Scale bars = 2 μm. *min* (') indicates the time point after IR of each displayed frame

(c) Select the "Source Channel" corresponding to the wavelength at which chromocenters were imaged (*i.e.*, RFP in this example), using the drop down menu.

(d) In the "Spot Detection" section, select 0.7 μm as "Estimated *XY* Diameter." Select the "Background

Subtraction" option. This value reliably detects most chromocenters, and can be lowered for smaller chromocenters.

(e) The algorithm will place spheres corresponding to all detected chromocenters. In the "Filters" section, select "Quality". Adjust the lowest threshold to a point at which the faintest chromocenters are reliably distinguished from the background throughout the kinetic.

(f) In the "Add/Delete (Cursor Intersects With)" section, using the drop down menu, select the "Specific Channel" corresponding to the wavelength at which chromocenters were imaged.

(g) In the "Algorithm" section, select the "Autoregressive Motion." In the "Parameters" section, change the "Max Distance" to 1–1.5 μm (higher numbers are used for cells displaying more mobility) and the "Max Gap Size" to 3. Select the box labeled "Fill gaps with all detected objects".

(h) Apply the filter "Track Duration" in the "Classify Tracks" section. Select and adjust the lower threshold to eliminate tracks that only last a few time points. Click the right pointing orange double arrow icon to finalize the track detection.

3. *Manual correction of chromocenter tracks.*

Tracks generated by Imaris may stop prematurely due to excessive photobleaching of smaller or dimmer signals, or include gaps where chromocenters were not detected, in which case automatically detected tracks require manual adjustments. This can be done by selecting the track of interest, and the specific time point that needs editing. To edit a track, select the corresponding spot and the "Edit Tracks" icon. Select the time point that requires editing, manually recreate a new spot, and connect it to the pre-existing track. Edit each track as necessary to assure that each chromocenter is tracked for as many time points as possible throughout the kinetic.

4. *Registration.*

Highlight all tracks and click the "Correct Drift" button below the tracks window. In the "Drift Correction Options," select "Translational And Rotational Drift." For the "Result Dataset Size" select "Include Entire Result." Confirm that the "Correct objects' positions" box is selected. Then, click "OK." Imaris will register the nucleus based on the selected tracks, which will compensate for any minor translational and rotational motion of the nucleus during the experiment (Fig. 5a). Save the resulting file with a new name. This will be used for further focus tracking.

3.2.10 Focus Tracking with Imaris

Tracking DNA damage foci is similar to the registration process, except that a new "spot" is generated for each tracked focus (Fig. 5b).

1. *Automated focus tracking.*
   Visually identify a focus for tracking. Repeat Subheading 3.2.9, **steps 2–4**, except that 0.3 μm should be selected as "Estimated XY Diameter" for foci. Additionally, select the "source channel" corresponding to the channel used for focus imaging (*i.e.,* GFP in this example). Most tracks are filtered out using both upper and lower thresholds for "Quality" and "Track Duration" filters, such that only the focus of interest remains tracked. Repeat this step as many times as necessary to track all foci under investigation.
2. *Manual correction of focus tracks.*
   Focus tracks generated by Imaris can result in large jumps to unrelated foci, especially when these are in close spatial proximity relative to the focus of interest, in which case tracks detected automatically require manual adjustments. To edit a track, select the corresponding spot and the "Edit Tracks" icon. Select the time point that requires editing, delete the spot at this time point, manually recreate a new spot, and connect it to the pre-existing track. Edit each track as necessary to assure that each focus is correctly identified throughout the kinetic.

3.2.11 Analysis of Focus Dynamics

Once tracks have been generated for individual foci, they can be used to extract positional data for biophysical analyses of focus motion, including MSD and LDM analyses. MSD analyses plot the average squared distance traveled by a focus at progressively increasing time intervals, providing quantitative measurements of the dynamic properties of focus motion [42, 64, 65]. MSD values are calculated across all time intervals to generate a curve for each track. MSD values across different foci are then averaged to describe the behavior of a population of foci. MSD curves can be used to calculate the average radius explored and the diffusion coefficient for a population of foci, and they enable distinguishing between Brownian, subdiffusive, and directed motions [42]. In a context of mixed types of motions (which typically characterize repair foci asynchronously moving in the nucleus), detection of directed motions requires more sophisticated analyses, including LDM detection [42] or alternative approaches [66, 67]. Here, we describe how to extract positional data from a population of foci tracked with Imaris. For the application of these data to MSD and LDM analyses, *see* previously published computational methods in Matlab and R, respectively [42].

1. *Extraction of positional data for biophysical analyses.*

For each tracked spot, select the "*Statistics*" tab and click on the "*Position*" information in the drop down menu of the "*Detailed*" tab. Click on the floppy disk icon to save the data as an excel file. The file contains three columns: posX, posY, and posZ, corresponding to the coordinates of the focus at each time point. To use MSD and LDM scripts provided in [42], add a column before these three and name it as "t". Number each time point with increasing number starting from "001" for the first time point, add the corresponding number at the beginning of each file name, and save this as a comma-separated value (.csv) file editable in Excel. Point to this file in the scripts for MSD and LDM calculations [42].

3.2.12 4D Image Rendering (Optional)

4D rendering of individual tracks relative to chromocenters and the nuclear periphery can be done in Imaris to facilitate the analysis and display of each track (Fig. 5). 4D rendering of chromocenters is obtained by generating volumes corresponding to HP1α signals. Using the "*Automatic Creation*" function, select the channel corresponding to HP1α and manually adjust smoothness and threshold to create volumes fitting this signal. Similarly, create a volume fitting the nuclear signal using the background signal derived from GFP-Mu2/Mdc1 (*see* **Note 11**). Finally, select the focus tracks of interest, and deselect the green and red channels of the original image before saving the image.

4 Notes

1. We do not recommend using Transit-Insect or Transit-2020 (Mirus) for transient transfection for live imaging, given the formation of fluorescent precipitates that interferes with the imaging procedure.
2. The use of *Drosophila* Kc cultured cells greatly facilitates live imaging experiments. *Drosophila* cells are maintained at room temperature and ambient CO_2 concentrations [68], which minimizes stress from environmental changes during cell culturing, sample processing, and live imaging.
3. The combination of filter sets and polychroic mirrors should be optimized for the tags of interest.
4. Transfections with up to three plasmids are highly efficient in *Drosophila* cells. However, transfections with 4+ plasmids result in most cells incorporating only three of the plasmids of interest.
5. Live cell imaging of nuclear F-actin can also be done 3–4 days after transient transfection. In this case, using greater amounts of plasmid DNA (10–12 μg) yields better results.

6. We attempted three color imaging of nuclear F-actin (F-actCB-mCitrin-NLS), heterochromatin (Aquamarine-HP1a), and damaged foci (mCh-Mu2/Mdc1). However, we found F-actCB-mCitrin-NLS to be insufficiently bright and photo-resistant for these experiments with the current imaging setup and conditions.
7. If cells are grown in the media with high autofluorescence (*e.g.,* Sf-900 II, Gibco), resuspend the cells in Schneider's media 10 min prior to the experiment to minimize autofluorescence.
8. After Equalization, files can also be batch processed using the "*Task Builder*" function, and specifying the parameters for deconvolution and volume rendering in the corresponding window.
9. We tested RFP-HP1α, RFP-HP1β and RFP-HP1γ as live markers for heterochromatin domains in NIH3T3 cells, and both RFP-HP1α and RFP-HP1β delivered a strong signal, with RFP-HP1α performing slightly better in our imaging conditions.
10. Live imaging of mouse cells expressing RFP-HP1α and GFP-MDC1 can also be done after transient transfection. In this case, we obtained the best transfection efficiency using electroporation. 10^6 cells are trypsinized, resuspended in 80 μl PBS 1×, and transferred in cuvettes for electroporation (Bulldog Bio, Cat. #12,358-346, 2 mm). Electroporation is done using a BioRad gene pulser with pulse controller, following the manufacturer's instructions. After electroporation, cells are incubated in cuvettes for 10 min and resuspended in 10% DMEM before seeding them in a chambered coverslip. Cells are imaged 48 h after electroporation.
11. Live markers for the nuclear periphery can also be used for this purpose (*see*, *e.g.*, [18]).

Acknowledgments

This work was supported by NIH R01GM117376 and NSF Career 1751197 to I.C., and NIH T32 GM118289 to C.S. We would like to thank S. Keagy for insightful comments on the chapter, S. Jackson, and P. Hemmerich for plasmids, the Longo lab for NIH3T3 cells, and C. Caridi for his help with MSD and LDM scripts.

Author contributions: C.S. contributed to optimizing imaging approaches and analysis methods in *Drosophila* cells, and D.A. in mouse cells. D.A., C.S., and I.C. wrote the manuscript. E.L. generated data for Fig. 2. *C.S. and D.A. contributed equally to this manuscript.

References

1. Peng JC, Karpen GH (2008) Epigenetic regulation of heterochromatic DNA stability. Curr Opin Genet Dev 18(2):204–211
2. Chiolo I, Tang J, Georgescu W et al (2013) Nuclear dynamics of radiation-induced foci in euchromatin and heterochromatin. Mutat Res 750(1–2):56–66
3. Amaral N, Ryu T, Li X et al (2017) Nuclear dynamics of heterochromatin repair. Trends Genet 33(2):86–100
4. Caridi PC, Delabaere L, Zapotoczny G et al (2017) And yet, it moves: nuclear and chromatin dynamics of a heterochromatic double-strand break. Philos Trans R Soc Lond Ser B Biol Sci 372(1731):pii: 20160291
5. Hoskins RA, Carlson JW, Kennedy C et al (2007) Sequence finishing and mapping of *Drosophila melanogaster* heterochromatin. Science 316(5831):1625–1628
6. Ho JW, Jung YL, Liu T et al (2014) Comparative analysis of metazoan chromatin organization. Nature 512(7515):449–452
7. Hoskins RA, Carlson JW, Wan KH et al (2015) The release 6 reference sequence of the *Drosophila melanogaster* genome. Genome Res 25 (3):445–458
8. James TC, Eissenberg JC, Craig C et al (1989) Distribution patterns of HP1, a heterochromatin-associated nonhistone chromosomal protein of Drosophila. Eur J Cell Biol 50(1):170–180
9. Riddle NC, Minoda A, Kharchenko PV et al (2011) Plasticity in patterns of histone modifications and chromosomal proteins in Drosophila heterochromatin. Genome Res 21 (2):147–163
10. Lachner M, O'Carroll D, Rea S et al (2001) Methylation of histone H3 lysine 9 creates a binding site for HP1 proteins. Nature 410 (6824):116–120
11. Dialynas GK, Terjung S, Brown JP et al (2007) Plasticity of HP1 proteins in mammalian cells. J Cell Sci 120(19):3415–3424
12. Horz W, Altenburger W (1981) Nucleotide sequence of mouse satellite DNA. Nucleic Acids Res 9(3):683–696
13. Ostromyshenskii DI, Chernyaeva EN, Kuznetsova IS et al (2018) Mouse chromocenters DNA content: sequencing and in silico analysis. BMC Genomics 19(1):151
14. Rawal C, Caridi PC, Chiolo I (2019) Actin' between phase separated domains for heterochromatin repair. DNA Repair. 81:102646
15. Kowalczykowski SC (2015) An overview of the molecular mechanisms of recombinational DNA repair. Cold Spring Harb Perspect Biol 7(11):pii: a016410
16. Peng JC, Karpen GH (2007) H3K9 methylation and RNA interference regulate nucleolar organization and repeated DNA stability. Nat Cell Biol 9(1):25–35
17. Peng JC, Karpen GH (2009) Heterochromatic genome stability requires regulators of histone H3 K9 methylation. PLoS Genet 5(3): e1000435
18. Ryu T, Spatola B, Delabaere L et al (2015) Heterochromatic breaks move to the nuclear periphery to continue recombinational repair. Nat Cell Biol 17(11):1401–1411
19. Ryu T, Bonner MR, Chiolo I (2016) Cervantes and Quijote protect heterochromatin from aberrant recombination and lead the way to the nuclear periphery. Nucleus 7(5):485–497
20. Caridi CP, D'Agostino C, Ryu T et al (2018) Nuclear F-actin and myosins drive relocalization of heterochromatic breaks. Nature 559 (7712):54–60
21. Dialynas G, Delabaere L, Chiolo I (2019) Arp2/3 and Unc45 maintain heterochromatin stability in Drosophila polytene chromosomes. Exp Biol Med. 244(15):1362–1371
22. Beucher A, Birraux J, Tchouandong L et al (2009) ATM and Artemis promote homologous recombination of radiation-induced DNA double-strand breaks in G2. EMBO J 28(21):3413–3427
23. Chiolo I, Minoda A, Colmenares SU et al (2011) Double-strand breaks in heterochromatin move outside of a dynamic HP1a domain to complete recombinational repair. Cell 144(5):732–744
24. Kakarougkas A, Ismail A, Klement K et al (2013) Opposing roles for 53BP1 during homologous recombination. Nucleic Acids Res 41(21):9719–9731
25. Janssen A, Breuer GA, Brinkman EK et al (2016) A single double-strand break system reveals repair dynamics and mechanisms in heterochromatin and euchromatin. Genes Dev 30 (14):1645–1657
26. Tsouroula K, Furst A, Rogier M et al (2016) Temporal and spatial uncoupling of DNA double strand break repair pathways within mammalian heterochromatin. Mol Cell 63 (2):293–305
27. Delabaere L, Chiolo I (2016) ReiNF4rcing repair pathway choice during cell cycle. Cell Cycle 15(9):1182–1183

28. Colmenares SU, Swenson JM, Langley SA et al (2017) Drosophila histone demethylase KDM4A has enzymatic and non-enzymatic roles in controlling heterochromatin integrity. Dev Cell 42(2):156–169 e5
29. Janssen A, Colmenares SU, Lee T et al (2019) Timely double-strand break repair and pathway choice in pericentromeric heterochromatin depend on the histone demethylase dKDM4A. Genes Dev 33(1–2):103–115
30. Caridi CP, Plessner M, Grosse R et al (2019) Nuclear actin filaments in DNA repair dynamics. Nat Cell Biol 21(9):1068–1077
31. Guenatri M, Bailly D, Maison C et al (2004) Mouse centric and pericentric satellite repeats form distinct functional heterochromatin. J Cell Biol 166(4):493–505
32. Li Q, Tjong H, Li X et al (2017) The three-dimensional genome organization of *Drosophila melanogaster* through data integration. Genome Biol 18(1):145
33. Jakob B, Splinter J, Conrad S et al (2011) DNA double-strand breaks in heterochromatin elicit fast repair protein recruitment, histone H2AX phosphorylation and relocation to euchromatin. Nucleic Acids Res 39(15):6489–6499
34. Haaf T, Golub EI, Reddy G et al (1995) Nuclear foci of mammalian Rad51 recombination protein in somatic cells after DNA damage and its localization in synaptonemal complexes. Proc Natl Acad Sci U S A 92(6):2298–2302
35. Maser RS, Monsen KJ, Nelms BE et al (1997) hMre11 and hRad50 nuclear foci are induced during the normal cellular response to DNA double-strand breaks. Mol Cell Biol 17 (10):6087–6096
36. Scully R, Chen J, Ochs RL et al (1997) Dynamic changes of BRCA1 subnuclear location and phosphorylation state are initiated by DNA damage. Cell 90(3):425–435
37. Liu Y, Li M, Lee EY et al (1999) Localization and dynamic relocalization of mammalian Rad52 during the cell cycle and in response to DNA damage. Curr Biol 9(17):975–978
38. Lisby M, Barlow JH, Burgess RC et al (2004) Choreography of the DNA damage response: spatiotemporal relationships among checkpoint and repair proteins. Cell 118 (6):699–713
39. Lisby M, Rothstein R (2004) DNA damage checkpoint and repair centers. Curr Opin Cell Biol 16(3):328–334
40. Costes SV, Chiolo I, Pluth JM et al (2010) Spatiotemporal characterization of ionizing radiation induced DNA damage foci and their relation to chromatin organization. Mutat Res 704(1–3):78–87
41. Delabaere L, Ertl HA, Massey DJ et al (2016) Aging impairs double-strand break repair by homologous recombination in Drosophila germ cells. Aging Cell. 16(2):320–328
42. Caridi CP, Delabaere L, Tjong H et al (2018) Quantitative methods to investigate the 4D dynamics of heterochromatic repair sites in Drosophila cells. Methods Enzymol 601:359–389
43. Stucki M, Clapperton JA, Mohammad D et al (2005) MDC1 directly binds phosphorylated histone H2AX to regulate cellular responses to DNA double-strand breaks. Cell 123 (7):1213–1226
44. Dronamraju R, Mason JM (2009) Recognition of double strand breaks by a mutator protein (MU2) in *Drosophila melanogaster*. PLoS Genet 5(5):e1000473
45. Madigan JP, Chotkowski HL, Glaser RL (2002) DNA double-strand break-induced phosphorylation of Drosophila histone variant H2Av helps prevent radiation-induced apoptosis. Nucleic Acids Res 30(17):3698–3705
46. Fernandez-Capetillo O, Lee A, Nussenzweig M et al (2004) H2AX: the histone guardian of the genome. DNA Repair 3(8–9):959–967
47. Wang B, Matsuoka S, Carpenter PB et al (2002) 53BP1, a mediator of the DNA damage checkpoint. Science 298(5597):1435–1438
48. Goldberg M, Stucki M, Falck J et al (2003) MDC1 is required for the intra-S-phase DNA damage checkpoint. Nature 421 (6926):952–956
49. Lou Z, Minter-Dykhouse K, Franco S et al (2006) MDC1 maintains genomic stability by participating in the amplification of ATM-dependent DNA damage signals. Mol Cell 21(2):187–200
50. Chapman JR, Jackson SP (2008) Phospho-dependent interactions between NBS1 and MDC1 mediate chromatin retention of the MRN complex at sites of DNA damage. EMBO Rep 9(8):795–801
51. Belin BJ, Cimini BA, Blackburn EH et al (2013) Visualization of actin filaments and monomers in somatic cell nuclei. Mol Biol Cell 24(7):982–994
52. Melak M, Plessner M, Grosse R (2017) Actin visualization at a glance. J Cell Sci 130 (3):525–530
53. Baarlink C, Wang H, Grosse R (2013) Nuclear actin network assembly by formins regulates the SRF coactivator MAL. Science 340 (6134):864–867
54. Belin BJ, Lee T, Mullins RD (2015) DNA damage induces nuclear actin filament assembly

by formin-2 and spire-(1/2) that promotes efficient DNA repair. Elife 4:e07735
55. Plessner M, Melak M, Chinchilla P et al (2015) Nuclear F-actin formation and reorganization upon cell spreading. J Biol Chem 290 (18):11209–11216
56. Iwaki T, Figuera M, Ploplis VA et al (2003) Rapid selection of Drosophila S2 cells with the puromycin resistance gene. Biotechniques 35(3):482–486
57. Ozaki T, Nagase T, Ichimiya S et al (2000) NFBD1/KIAA0170 is a novel nuclear transcriptional transactivator with BRCT domain. DNA Cell Biol 19(8):475–485
58. Galanty Y, Belotserkovskaya R, Coates J et al (2009) Mammalian SUMO E3-ligases PIAS1 and PIAS4 promote responses to DNA double-strand breaks. Nature 462(7275):935–939
59. Schmiedeberg L, Weisshart K, Diekmann S et al (2004) High- and low-mobility populations of HP1 in heterochromatin of mammalian cells. Mol Biol Cell 15(6):2819–2833
60. Riedl J, Crevenna AH, Kessenbrock K et al (2008) Lifeact: a versatile marker to visualize F-actin. Nat Methods 5(7):605–607
61. Johnson HW, Schell MJ (2009) Neuronal IP3 3-kinase is an F-actin-bundling protein: role in dendritic targeting and regulation of spine morphology. Mol Biol Cell 20(24):5166–5180
62. Burkel BM, von Dassow G, Bement WM (2007) Versatile fluorescent probes for actin filaments based on the actin-binding domain of utrophin. Cell Motil Cytoskeleton 64 (11):822–832
63. Goodarzi AA, Noon AT, Deckbar D et al (2008) ATM signaling facilitates repair of DNA double-strand breaks associated with heterochromatin. Mol Cell 31(2):167–177
64. Saxton MJ, Jacobson K (1997) Single-particle tracking: applications to membrane dynamics. Annu Rev Biophys Biomol Struct 26:373–399
65. Spichal M, Fabre E (2017) The emerging role of the cytoskeleton in chromosome dynamics. Front Genet 8:60
66. Lamm N, Masamsetti VP, Read MN et al (2018) ATR and mTOR regulate F-actin to alter nuclear architecture and repair replication stress. bioRxiv. https://doi.org/10.1101/451708
67. Oshidari R, Strecker J, Chung DKC et al (2018) Nuclear microtubule filaments mediate non-linear directional motion of chromatin and promote DNA repair. Nat Commun 9 (1):2567
68. Cherbas L, Gong L (2014) Cell lines. Methods 68(1):74–81
69. Ayoub N, Jeyasekharan AD, Bernal JA et al (2008) HP1-beta mobilization promotes chromatin changes that initiate the DNA damage response. Nature 453(7195):682–686